

# Independence of Inductive kick on Inductance of a Pulse Induction Circuit

Olanrewaju WOJUOLA

Department of Physics, North-West University, South Africa

o.wojuola@ieee.org

**Abstract**— It is commonly believed that inductive kick or back electromotive force (EMF) generated by a coil depends on the magnitude of its inductance. This, intuitively, is in line with Faraday's law of electromagnetic induction. This work seeks to show that this is not necessarily the case. Starting from basic principles, this work presents a theoretical analysis which shows that the back EMF generated by a pulse induction coil does not depend on inductance. Rather, the back EMF is a function of the ratio of the load to the coil resistance. The theoretical analysis is supported with results of circuit simulation confirming the independence of the back EMF on inductance.

**Keywords**- Inductive kick, back EMF, pulse induction coil, back EMF, Lenz's law, Faraday's law of electromagnetic induction, inductance

## I. INTRODUCTION

Pulse induction is an important technique used in metal detectors [1] [2] [3] [4], an essential tool that finds practical application in non-destructive testing of concrete [5] [6] [7] [8] [9], subsurface discrimination [10], landmine detection [11] [12] and detection of metal shrapnel during surgery [13], among others. The initial interest in the pulse induction circuit originated from the authors' desire to investigate the possibility of using pulse induction technique for non-destructive evaluation of a reinforced concrete structure. However, the present focus is to have a close look at the fundamental behaviour of the circuit. The pulse induction circuit being considered basically comprises a coil connected in parallel to a resistive load (Figure 1). The circuit is very simple, but is known to exhibit remarkable behaviour, exemplified as follows. The first example relates to the use of the circuit for demonstrating back EMF in the physics laboratory [14-16], for which the load  $R_L$  is a bulb (Figure 2a). As an illustration, assume that the load is a 60 V bulb connected to a 12 V battery. With the switch closed, the bulb burns dimly. However, opening the switch sends a flash of light through the bulb. The same circuit is known to be capable of generating a spark across a gap (Figure 2b). These behaviours are remarkable in that the circuit can exhibit them even when operated from a low voltage DC source.

For the circuit, intuition suggests that when the switch is opened, the magnitude of the back EMF generated by the coil should be directly proportional to coil's inductance, according to Faraday's law of electromagnetic induction. In contrast however, simple analysis to be presented here shows that the back EMF does not depend on the inductance of the coil.

Instead, the back EMF is a function of the ratio of the load to the coil resistance. The bigger the ratio, the higher the back EMF generated by the coil. Furthermore, the simple analysis shows that the coil will not necessarily generate a *huge* back EMF: depending on the ratio of the coil to the load resistance, it is possible for the back EMF to be less than the supply voltage. This paper gives a close look at the behaviour of the circuit.

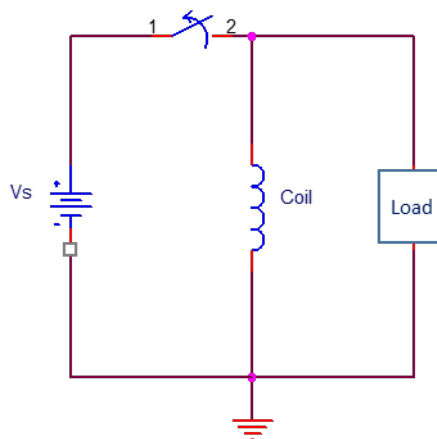


Figure 1. The pulse induction circuit

## II. FUNDAMENTAL THEORY

Every real coil possesses some intrinsic resistance, so that the coil may be modelled as an inductor in series with a resistor. Therefore, the pulse induction circuit (Figure 1) may be equivalently represented by Figure 3, where  $L_c$  and  $R_c$  represent the inductance and the resistance of the coil respectively. Looking at it ordinarily, the circuit is a simple RL-R transient circuit. However, the focus of the present effort is not just in the transient behaviour of the circuit, but to examine the circuit's ability to generate a huge back EMF from a relatively low voltage source.

It should be noted that the primary interest is in the behaviour of the circuit when the switch is cut OFF, because it is at that instant that the back EMF is generated. That is to say, the real interest is in what happens during the signal's decay cycle. For completeness however, not only the decay cycle but also the rise cycle of the circuit shall be described. We will now begin with the basic theory of the circuit's transient response.

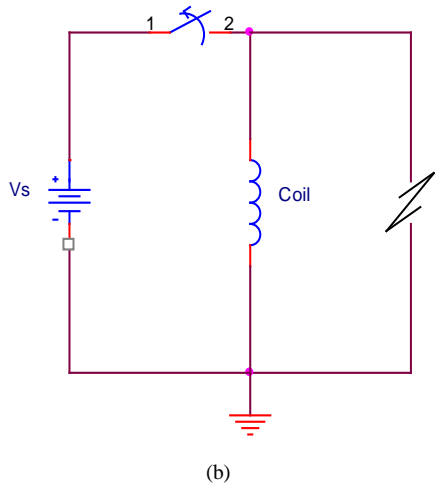
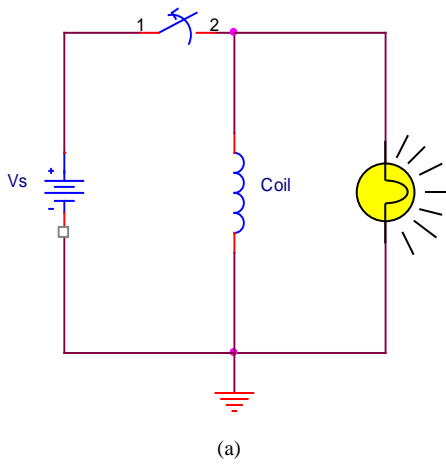


Figure 2. Examples of remarkable behaviour of the inductor-driven pulse induction circuit: (a) The flash-bulb experiment – opening the switch sends a flash of light through the bulb; (b) Generation of a spark across a gap - opening the switch generates a spark across the gap.

With the switch connected, the voltage source  $V_s$  drives a steady current  $I_L$  through load  $R_L$ , where  $I_L = \frac{V_s}{R_L}$ ; and an exponential current  $i_c$  through the coil:

$$i_c(t) = I_c \left( 1 - e^{-\frac{t}{\tau_r}} \right) \quad (1)$$

where rise time constant,  $\tau_r = L_c/R_c$ ; and the steady state current  $I_c = V_s/R_c$ . The instantaneous voltage  $v_{Lc}$  across the inductance  $L_c$  is given by

$$v_{Lc} = V_s e^{-\frac{t}{\tau_r}} \quad (2)$$

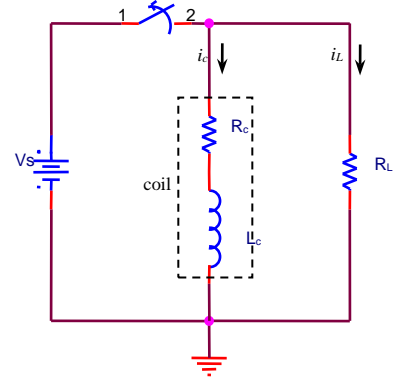


Figure 3. The replacement of the coil by its equivalent circuit elements

Now assume that the circuit is in a steady state. Opening the switch disconnects the battery, thereby sending the applied voltage to zero. The current decays exponentially according to the relation

$$i_c(t) = I_c e^{-\frac{t}{\tau_f}}; \quad \tau_f = \frac{L_c}{R_c + R_L} \quad (3)$$

where  $\tau_f$  is the signal's fall (decay) time constant. The voltage across the inductance is given by

$$v_{Lc}(t) = -V_s \left( \frac{R_c + R_L}{R_c} \right) e^{-\frac{t}{\tau_f}} \quad (4)$$

Waveforms for the voltages and the currents associated with the pulse induction circuit may be expressed as:

$$v_{Lc}(t) = \sum_{n=0}^{\infty} \bar{v}_{Lc}(t - n(T_m + T_s)) U(t - n(T_m + T_s)) \quad (5)$$

where

$$\bar{v}_{Lc}(t) = V_s \left\{ \begin{aligned} & e^{-\frac{t}{\tau_r}} [U(t) - U(t - T_m)] - \left( \frac{R_c + R_L}{R_c} e^{-\frac{(t-T_m)}{\tau_f}} \right) \\ & [U(t - T_m) - U(t - (T_m + T_s))] \end{aligned} \right\} \quad (6)$$

$v_{Lc}$  is voltage across the inductance  $L_c$ ,  $\bar{v}_{Lc}(t)$  defines a complete cycle of the signal waveform, while the former function  $v_{Lc}(t)$  specifies the periodicity of the waveform;  $v_{rw}$  is a rectangular wave train having a mark and a space  $T_m$  and  $T_s$  respectively. The rectangular waveform drives the switch which undergoes a repetitive ON-OFF cycle of duration  $T_m$  and  $T_s$  respectively. The upper limit of the former function means that the waveform is free-running (repeats endlessly). It can be shown also that the waveform of  $i_c$  can be represented as:

$$i_c(t) = \sum_{n=0}^{\infty} \bar{i}_c(t - n(T_m + T_s)) U(t - n(T_m + T_s)) \quad (7)$$

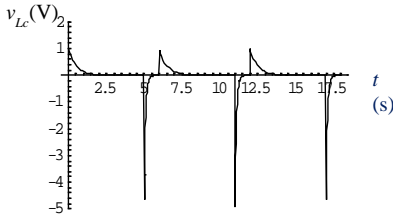
where

$$\bar{i}_c(t) = I_c \left\{ \begin{aligned} & \left(1 - e^{-\frac{t}{\tau_r}}\right) [U(t) - U(t - T_m)] + \left(e^{-\frac{(t-T_m)}{\tau_f}}\right) \\ & [U(t - T_m) - U(t - (T_m + T_s))] \end{aligned} \right\} \quad (8)$$

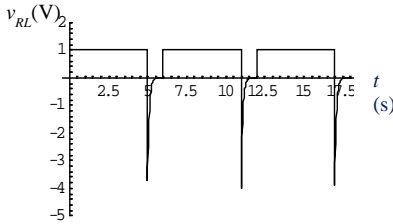
### III. IMPORTANT OBSERVATION

There is a simple but important observation concerning the back EMF generated by the coil. Considering the Faraday's law ( $e = -L \frac{di}{dt}$ ), intuition suggests that the magnitude of the back EMF should be proportional to inductance. In contrast, Equation 4 shows the contrary. Looking at this equation, it can be seen that peak back EMF across the coil is given by:

$$E_b = - \left(1 + \frac{R_L}{R_c}\right) V_s$$



(a)

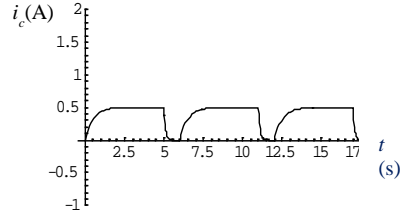


(c)

This equation shows that the magnitude of the back EMF depends neither on the inductance of the coil, nor the rate of decay of the current. Rather, it is a function of the ratio of the load to the coil resistance. The bigger the ratio, the higher the back EMF. More will be said about this point later.

### IV. RESULTS

Software simulations were carried out to confirm the independence of the magnitude of the back EMF on the inductance of the coil. Figure 4 the circuit shows three cycles of the circuit's signals, obtained by direct software implementation of equations 6 to 9. The figure clearly indicates the periodicity of the waveforms. PSPICE transient simulations were also carried out for different sets of component values. To ensure that the signals reach steady state before switching over to the next phase, the following were assumed for the mark  $T_m$  and the space  $T_s$ :  $T_m = 10\tau_r$ ,  $T_s = 10\tau_f$ . These values give enough steady state interval to make the signal's rise cycle distinct from its decay. The circuit components were declared as global parameters and parametric traces were generated for the signals. Parametric traces were obtained for voltage  $v_{Lc}$  across the inductance  $L_c$  for a range of values of each of the components. Without loss of generality, simple component values were used for easy assessment of the results. Figure 5 shows an example of the parametric traces, with the coil inductance  $L_c$  as parameter.  $L_c$  was swept over the values 0.1, 0.5, 1.0, 1.5 and 2 H;  $R_L$  and  $R_c$  were kept at default values of 8  $\Omega$  and 2  $\Omega$  respectively.



(b)

Figure 4. Multiple-cycle signal waveforms for the pulse induction circuit, obtained by direct software implementation of the analytic expressions for the waveforms.

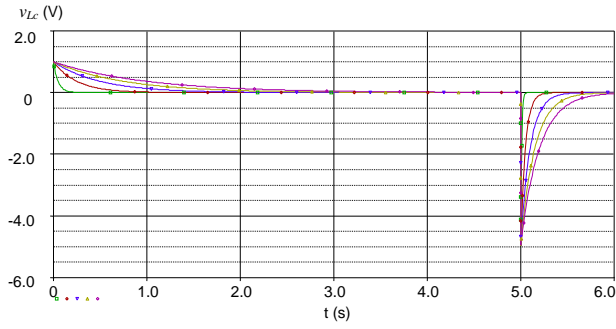


Figure 5. Parametric traces of the voltage  $v_{L_c}$  for different values of the coil inductance  $L_c$ .

Sets of data were extracted and these were used to generate parametric graphs. Table 1 is an example of a set of extracted data. This array of data was obtained from 6 families of parametric traces, one family for each value of  $R_c$ .

TABLE I. TABLE 1. A TYPICAL EXAMPLE OF THE TABLE OF VALUES OF THE PEAKS THAT WERE EXTRACTED FROM THE PARAMETRIC TRACES

$R_L (\Omega)$	$E_b (V)$					
	$R_c = 2\Omega$	$R_c = 4\Omega$	$R_c = 6\Omega$	$R_c = 8\Omega$	$R_c = 10\Omega$	$R_c = 12\Omega$
2	-1.9801	-1.4888	-1.3245	-1.2422	-1.1928	-1.1599
4	-2.9775	-1.9900	-1.6597	-1.4944	-1.3951	-1.3289
6	-3.9733	-2.4896	-1.9933	-1.7449	-1.5957	-1.4963
8	-4.9887	-2.9888	-2.3265	-1.9950	-1.7959	-1.6632
10	-5.9639	-3.4878	-2.6596	-2.2449	-1.9960	-1.8300
12	-6.9591	-3.9867	-2.9925	-2.4948	-2.1960	-1.9967

#### A. Dependence of back EMF on load and coil resistance

Figure 6 shows the parametric graphs of the peak EMF  $E_b$  against  $R_L$ , with  $R_c$  as a parameter.  $L_c$  was kept at a fixed value. A close look at this figure shows that  $E_b$  is linearly proportional to  $R_L$ , with a slope  $1/R_c$ . This is consistent with Equation 5, thus confirming the dependence of the back EMF on the resistors  $R_L$  and  $R_c$ .

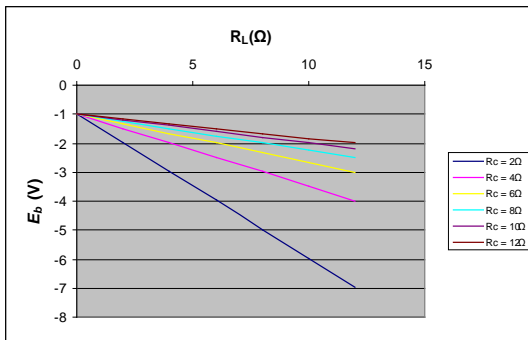


Figure 6. Parametric graphs showing the dependence of the back EMF  $E_b$  on the load  $R_L$  and the coil resistance  $R_c$ .

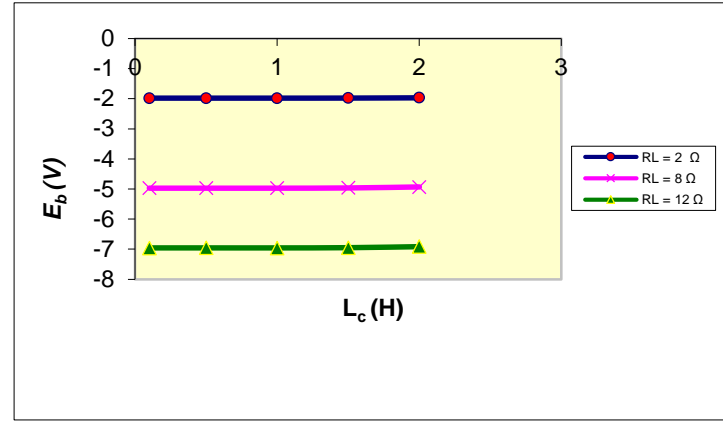


Figure 7. Independence of the peak back emf  $E_b$  on the coil inductance  $L_c$ . This graph shows parametric plot of  $E_b$  against  $L_c$  for different values of the load  $R_L$ .

#### B. Independence of back EMF on inductance

Figure 7 shows the parametric graphs of back EMF  $E_b$  against inductance  $L_c$ , with  $R_L$  as a parameter.  $R_c$  was kept at a fixed value. Looking at this figure, it is obvious that the back EMF does not depend on the coil inductance.

## V. DISCUSSION

Using a simple analysis, attempt is made here to explain why back EMF generated by the coil does not depend on inductance. As mentioned earlier, the back EMF generated by the coil is in accordance to the relationship:

$$e_b = -L_c \frac{di_c}{dt}$$

Intuition suggests that the magnitude of the back EMF should depend on the inductance. However, this is not the case. The reason for this is explained as follows. During the signal decay, the coil current  $i_c$  decays according to Equation 3. Substituting for  $i_c$  in the previous equation and evaluating gives

$$e_b = L_c \left( \frac{1}{\tau_f} I_c e^{-\frac{t}{\tau_f}} \right)$$

Comparing the last two equations, it is obvious that the expression in the brackets of the latter equation represents the rate of change of the current  $i_c$ . This implies that the rate of change of the current is inversely proportional to the time constant  $\tau_f$ . Now since  $\tau_f \propto L_c$ , it means that if inductance increases, the rate of change of the current will decrease proportionally. This leads to self-cancellation: the effect (benefit) of increasing the inductance is nullified by corresponding decrease in the rate of change of the current. Consequently, change in the inductance has no effect on the magnitude of the back EMF.

## VI. CONCLUSION

This paper considered the behaviour of a pulse induction circuit commonly used for demonstrating back EMF in the physics laboratory. This paper showed back EMF generated by the coil depends neither on inductance nor the rate of decay of the pulse signal, but on the ratio of the load to the coil resistance. The coil will not necessarily generate a huge back EMF: depending on the ratio of the load to the coil resistance, it is possible for the back EMF to be less than the supply voltage.

## ACKNOWLEDGMENT

The author expresses gratitude to the North-West University for providing funds for participating in the SAIP conference.

## REFERENCES

- [1] D. Ambruš, D. Vasić, and V. Bilas, "Model-based target classification using spatial and temporal features of metal detector response," in *2015 IEEE Sensors Applications Symposium (SAS)*, 2015, pp. 1-6.
- [2] B. Kim, S. Han, and K. Kim, "Planar Spiral Coil Design for a Pulsed Induction Metal Detector to Improve the Sensitivities," *IEEE Antennas and Wireless Propagation Letters*, vol. 13, pp. 1501-1504, 2014.
- [3] A. Rerkratn, W. Petchmaneelumka, J. Kongkauropham, K. Krajsoda, and A. Kaewpoonsuk, "Pulse Induction Metal Detector Using Sample and Hold Method," in *2011 11th International Conference on Control, Automation and Systems*, 2011, pp. 45-48.
- [4] J. A. Vega and A. G. S., "On the Signal Features Analysis of a Pulse Induction Metal Detector Prototype," in *2012 Spring Congress on Engineering and Technology*, 2012, pp. 1-4.
- [5] M. Bartholmai, S. Johann, M. Kammermeier, M. Mueller, and C. Strangfeld, "Transmission characteristics of RFID sensor systems embedded in concrete," in *2016 IEEE SENSORS*, 2016, pp. 1-3.
- [6] J. T. Bernhard, K. Hietpas, E. George, D. Kuchima, and H. Reis, "An interdisciplinary effort to develop a wireless embedded sensor system to monitor and assess corrosion in the tendons of prestressed concrete girders," in *2003 IEEE Topical Conference on Wireless Communication Technology*, 2003, pp. 241-243.
- [7] X. Dérobert, G. Villain, and A. Ihamouten, "Recent developments of EM non-destructive testing in the radar frequency-band for the evaluation of cover concretes," in *2015 European Radar Conference (EuRAD)*, 2015, pp. 233-236.
- [8] P. K. Frankowski, "Corrosion detection and measurement using eddy current method," in *2018 International Interdisciplinary PhD Workshop (IIPhDW)*, 2018, pp. 398-400.
- [9] M. Kubo, M. Okamoto, and J. Takayama, "Non-destructive inspection of buried object in concrete structures based on improved propagation path model using microwave radar," in *2017 56th Annual Conference of the Society of Instrument and Control Engineers of Japan (SICE)*, 2017, pp. 695-698.
- [10] T. Bell and B. Barrow, "Subsurface discrimination using handheld electromagnetic induction sensors," in *IGARSS 2000. IEEE 2000 International Geoscience and Remote Sensing Symposium. Taking the Pulse of the Planet: The Role of Remote Sensing in Managing the Environment. Proceedings (Cat. No.00CH37120)*, 2000, vol. 4, pp. 1433-1435 vol.4.
- [11] B. Kim, J. W. Yoon, S. Lee, S. Han, and K. Kim, "Pulse-induction metal detector with time-domain bucking circuit for landmine detection," *Electronics Letters*, vol. 51, no. 2, pp. 159-161, 2015.
- [12] C. Rennie, B. Arendse, M. R. Inggs, and A. Langman, "Practical measurements of land mine simulants using a SFCW radar, a pulse induction metal detector and an infrared camera," in *1998 Second International Conference on the Detection of Abandoned Land Mines (IEE Conf. Publ. No. 458)*, 1998, pp. 182-186.
- [13] M. Sakthivel, B. George, V. J., and M. Sivaprakasam, "A new inductive proximity sensor as a guiding tool for removing metal shrapnel during surgery," in *2013 IEEE International Instrumentation and Measurement Technology Conference (I2MTC)*, 2013, pp. 53-57.
- [14] A. Grohmann, S. Beschaffung, and D. Plano. (10 Nov 2019). *Back EMF - inductors, back EMF and Lenz's law*. Available: <https://sciencedemonstrations.fas.harvard.edu/presentations/back-emf>
- [15] Physics Dept Brown Univ. (10 Nov 2019). *Back EMF*. Available: <https://wiki.brown.edu/confluence/display/PhysicsLabs/5J10.23+B+ack+emf>
- [16] Physics Dept NCSU. (10 Nov 2019). *Back emf*. Available: <http://demoroom.physics.ncsu.edu/html/demos/381.html>